

Understanding future patterns of increased precipitation intensity in climate model simulations

Gerald A. Meehl,¹ Julie M. Arblaster,^{1,2} and Claudia Tebaldi¹

Received 31 May 2005; revised 4 August 2005; accepted 25 August 2005; published 30 September 2005.

[1] In a future climate warmed by increased greenhouse gases, increases of precipitation intensity do not have a uniform spatial distribution. Here we analyze a multi-model AOGCM data set to examine processes that produce the geographic pattern of these precipitation intensity changes over land. In the tropics, general increases in water vapor associated with positive SST anomalies in the warmer climate produce increased precipitation intensity over most land areas. In the midlatitudes, the pattern of precipitation intensity increase is related in part to the increased water vapor being carried to areas of mean moisture convergence to produce greater precipitation, as well as to changes in atmospheric circulation. Advective effects, indicated by sea level pressure changes, contribute to greatest precipitation intensity increases (as well as mean precipitation increases) over northwestern and northeastern North America, northern Europe, northern Asia, the east coast of Asia, southeastern Australia, and south-central South America. **Citation:** Meehl, G. A., J. M. Arblaster, and C. Tebaldi (2005), Understanding future patterns of increased precipitation intensity in climate model simulations, *Geophys. Res. Lett.*, 32, L18719, doi:10.1029/2005GL023680.

1. Introduction

[2] It has been widely reported that in a warmer future climate with increased greenhouse gases (GHGs), model simulations show a general increase in precipitation intensity, that is, relatively more precipitation falls in a given daily precipitation event [e.g., Cubasch *et al.*, 2001; Palmer and Räisänen, 2002; Semenov and Bengtsson, 2002; Voss *et al.*, 2002; Milly *et al.*, 2002; Watterson and Dix, 2003; Wehner, 2004; Räisänen, 2005]. Some earlier studies on changes of extremes, such as changes of frost days [Meehl *et al.*, 2004] and changes in heat waves [Meehl and Tebaldi, 2004] have shown the importance of changes in atmospheric circulation and advection to the pattern of changes in extremes.

[3] C. Tebaldi *et al.* (Going to the extremes: An inter-comparison of model-simulated historical and future changes in extreme events, submitted to *Climatic Change*, 2005, hereinafter referred to as Tebaldi *et al.*, submitted manuscript, 2005) have analyzed the ten extremes indices of Frich *et al.* [2002] as computed by nine AOGCMs for climate change simulations in the 21st century for the IPCC

Fourth Assessment Report. Of those ten indices, five relate to precipitation extremes, and four of those relate to changes in precipitation intensity in one form or another. Here we examine one of the precipitation indices, the “simple daily intensity index” (termed “precip intensity” by Tebaldi *et al.* and used here as well), defined as the total annual precipitation amount divided by the total number of wet days in the year. As shown by Tebaldi *et al.* (submitted manuscript, 2005), precip intensity is qualitatively representative of the other precipitation extremes indices, and all the changes in precipitation extremes indices show roughly the same pattern. Therefore, choosing precip intensity is useful as a starting point to analyze processes associated with producing the geographic patterns of changes in precipitation extremes.

[4] As noted above, nine modeling groups have calculated the extremes indices, and those nine models are analyzed here. The models are: PCM, CCSM3, GFDL-CM2.0, GFDL-CM2.1, MIROC3.2-hires, MIROC3.2-medres, CNRM-CM3, MRI-CGCM2.3.2, and INMCM3_0. A more full description of the models as well as additional details regarding the multi-model archive can be found at: http://www.pcmdi.llnl.gov/ipcc/about_ipcc.php.

[5] In this study we analyze results for the end of the 21st century for the SRES A1B scenario (a mid-range positive radiative forcing scenario [see Meehl *et al.*, 2005]). Geographical patterns for other scenarios were found to be nearly the same. All differences are calculated as annual mean values for the years 2080–2099 minus 1980–1999.

2. Patterns of Changes in Extreme Precipitation

[6] Figure 1 shows the multi-model ensemble mean change in precip intensity over land areas for the multi-model ensemble mean difference for the end of the 21st century after Tebaldi *et al.* (submitted manuscript, 2005). The individual models’ patterns have been first normalized with respect to the standard deviation of the detrended time series computed at each individual gridpoint over the 1960–2099 period, in order to correct for the different absolute magnitudes of the changes and focus on the sign and significance of them. Stippling indicates areas where at least four of the models, out of the nine total, agree on the sign and significance of the difference. There are other ways to present these data, such as showing percent changes. However, that technique produces disproportionately large changes in arid areas where a relatively small increase in absolute precipitation can result in a huge percent change, thus complicating the interpretation in a multi-model analysis. There are limitations with other methods as well, but the normalization by respective

¹National Center for Atmospheric Research, Boulder, Colorado, USA.

²Also at Bureau of Meteorology Research Centre, Melbourne, Victoria, Australia.

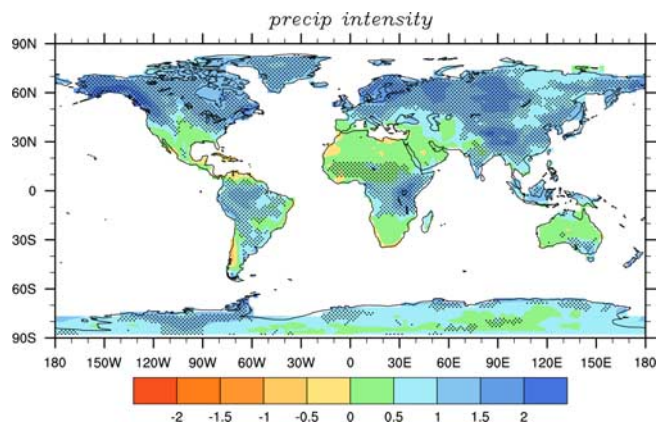


Figure 1. The nine member multi-model ensemble mean precip intensity difference after Tebaldi et al. (submitted manuscript, 2005) for A1B, 2080–2099 minus 1980–1999 (time series were normalized by the de-trended 1960–2099 standard deviation, and are in units of standard deviation). As by Tebaldi et al. (submitted manuscript, 2005) stippling denotes areas where at least four of the nine models have a statistically significant change.

de-trended standard deviations puts the models on more comparable terms in comparing the changes in units of standard deviations in Figure 1.

[7] A new gridded data set of observed changes in precipitation indices is nearly ready for release (L. Alexander, personal communication), and a detailed comparison of the multi-model simulations of 20th century extremes awaits that data set to be available. However, Kiktev et al. [2003] have looked at one model simulation of precipitation intensity and found the pattern of variability during 20th century

to be close to observations, but the observed trends in precipitation intensity were not captured well by that model (atmosphere-only run with observed SSTs). Simulation of such trends in the coupled models analyzed here will be compared to this observed data set when it becomes available.

[8] Though almost all areas in Figure 1 show increases in precip intensity (positive differences) for this multi-model mean, there is a distinct pattern to the changes. Increases of precipitation intensity are greatest in the tropics, as well as over northern Europe, northern Asia, the east coast of Asia, northwestern and northeastern North America, southwestern Australia, and parts of south-central South America.

[9] Figure 2a shows the surface temperature differences associated with the changes in precipitation intensity. As is the case in these transient simulations [e.g., Cubasch et al., 2001], high latitudes and land areas show greater warming than the oceans, with the tropical oceans and particularly the tropical Pacific showing somewhat greater values of warming compared to other ocean areas. These changes in tropical SSTs and associated increased evaporation, as well as the warmer atmospheric temperatures that allow the air to hold more moisture, combine to produce increased water vapor in the atmosphere (Figure 2b). The greatest absolute increases in water vapor occur in the tropics, and this contributes directly to the increases of tropical precipitation seen in Figure 2c. In the midlatitudes, the general increases in water vapor certainly contribute to increased mean precipitation. But another factor is that in areas of mean moisture convergence in present-day climate (not shown), there are increases in mean precipitation in the warmer climate simply due to the warmer air holding more moisture. This relationship was mentioned in the first IPCC assessment in 1991, and has more recently been quantified

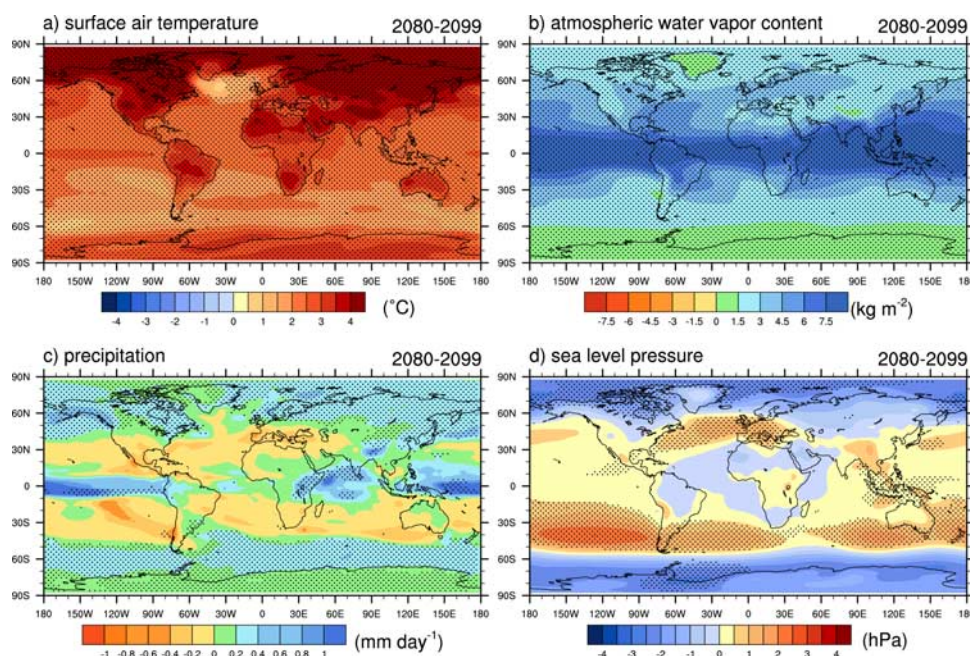


Figure 2. (a) annual mean surface temperature differences, °C, 2080–99 minus 1980–99, for A1B from the nine member multi-model ensemble; (b) same as Figure 2a except for vertically integrated water vapor differences, kg m^{-2} ; (c) same as Figure 2a except for precipitation differences (mm day^{-1}); (d) same as Figure 2a except for SLP differences (hPa). Dotted regions denote where the multi-model ensemble mean divided by the inter-model standard deviation exceeds one.

by Watterson [1998]. Emori and Brown [2005] have also illustrated this effect such that for comparable vertical motion regimes, more intense precipitation is simulated in a future warmer climate.

[10] The increases in water vapor and moisture convergence are reflected in increases in mean precipitation (Figure 2c) in most areas of the tropics, northern Europe, northern Asia, the east coast of Asia, northwest and northeast North America, southeastern Australia, and parts of south-central South America. Note these areas correspond to the same areas of increased precip intensity noted in Figure 1. Therefore, there is an association between the geographic areas of increases in mean precipitation and similar areas of increases of precip intensity [e.g., Räisänen, 2005]. To illustrate this association, the pattern correlation between changes in mean precipitation and precipitation intensity is +0.6 (pattern correlation calculated for all grid points). There are also some areas where precipitation intensity increases and mean precipitation decreases (e.g. southwest U.S., Mediterranean region). This is related in part to longer periods of dry days between precipitation events in those areas (Tebaldi et al., submitted manuscript, 2005).

[11] To further understand what is contributing to these patterns of change related to advection, it is useful to look at differences in sea level pressure (SLP) in Figure 2d. For the multi-model mean, changes in SLP show decreases at high latitudes and increases in parts of the midlatitudes and subtropics. Part of this is due to a poleward shift of the storm tracks in each hemisphere [e.g., Yin, 2005], with an intensification of the southern westerlies associated with a deeper circumpolar trough over the southern oceans with increased GHGs [Arblaster and Meehl, 2005]. Negative SLP anomalies are seen over the northern North Atlantic, northern Asia, the northern North Pacific and northeastern North America.

[12] The changes in precipitation in the subtropics and high latitudes (Figures 2b and 2c) are affected by the changes in quasi-geostrophic circulation implied by the SLP anomalies. The negative SLP anomalies over the North Atlantic, northern Asia, the north Pacific and northeastern North America are associated with anomalous southwesterly flow across the North Pacific, North Atlantic, and northwest Asia (not shown). Meanwhile, negative SLP anomalies near southeast Australia and over south-central South America produce anomalous northwesterly flow over those regions. These low level atmospheric circulation anomalies bring relatively more water vapor from warmer, more moist regions to the midlatitudes, and these midlatitude areas then experience greater increases of mean precipitation (Figure 2c) and corresponding increases of precipitation intensity (Figure 1).

3. Conclusions

[13] A nine member multi-model ensemble is analyzed to understand the pattern of increased precipitation intensity with increased GHGs. Results are shown for the intermediate forcing scenario, A1B, and are illustrative of the other SRES scenarios. Warmer tropical SSTs with increased GHGs produce relatively large increases in water vapor due to increased evaporation, and consequently a general increase in tropical precipitation and increased precip

intensity. At higher latitudes, in addition to increases in water vapor producing more precipitation in regions of climatological moisture convergence, advective effects associated with changes in atmospheric circulation produce greater precip intensity increases over northwestern and northeastern North America, northern Europe, northern Asia, the east coast of Asia, southeastern Australia, and south-central South America. That is, there is low level moisture convergence that produces increases in mean as well as extreme precipitation in these regions. Such changes in low level moisture convergence for the 20 year averaging intervals we consider here are nearly comparable to changes in precipitation minus evaporation [e.g., Simmonds et al., 1999], and the pattern of those changes in low level moisture convergence and P-E (not shown) look very similar to the precip intensity and mean precipitation differences in Figure 2c [e.g., Räisänen, 2005].

[14] The pattern of changes in precip intensity in a future warmer world is related to the increases of water vapor. Areas with increased water vapor imply that the air is holding more moisture, so that for a given precipitation event, more precipitation falls, thus producing an increase in precip intensity [see also Emori and Brown, 2005]. In the tropics, there is simply more water vapor almost everywhere evaporating from the warmer oceans, and precip intensity increases over most tropical continental areas. For the midlatitudes, there is a link between changes in low level circulation, represented here by changes in SLP, and the pattern of changes in precip intensity. Some of these changes in atmospheric circulation are caused by a poleward shift in the storm tracks with increases GHGs [Yin, 2005].

[15] **Acknowledgments.** We acknowledge the international modeling groups for providing their data for analysis, the Program for Climate Model Diagnosis and Intercomparison (PCMDI) for collecting and archiving the model data, the JSC/CLIVAR Working Group on Coupled Modelling (WGCM) and their Coupled Model Intercomparison Project (CMIP) and Climate Simulation Panel for organizing the model data analysis activity, and the IPCC WG1 TSU for technical support. The IPCC Data Archive at Lawrence Livermore National Laboratory is supported by the Office of Science, U.S. Department of Energy. Portions of this study were supported by the Office of Biological and Environmental Research, U.S. Department of Energy, as part of its Climate Change Prediction Program, and the National Center for Atmospheric Research. This work was also supported in part by the Weather and Climate Impact Assessment Initiative at the National Center for Atmospheric Research. The National Center for Atmospheric Research is sponsored by the National Science Foundation.

References

- Arblaster, J. M., and G. A. Meehl (2005), Contribution of various external forcings to trends in the Southern Annular Mode, *J. Clim.*, in press.
- Cubasch, U., G. A. Meehl, G. J. Boer, R. J. Stouffer, M. Dix, A. Noda, C. A. Senior, S. Raper, and K. S. Yap (2001), Projections of future climate change, in *Climate Change 2001: The Scientific Basis: Contribution of Working Group I to the Third Assessment Report of the Intergovernmental Panel on Climate Change*, edited by J. T. Houghton et al., pp. 525–582, Cambridge Univ. Press, New York.
- Emori, S., and S. J. Brown (2005), Dynamic and thermodynamic changes in mean and extreme precipitation under changed climate, *Geophys. Res. Lett.*, *32*, L17706, doi:10.1029/2005GL023272.
- Frich, P., L. V. Alexander, P. Della-Marta, B. Gleason, M. Haylock, A. M. G. Klein Tank, and T. Peterson (2002), Observed coherent changes in climatic extremes during the second half of the twentieth century, *Clim. Res.*, *19*, 193–212.
- Kiktev, D., D. M. H. Sexton, L. Alexander, and C. K. Folland (2003), Comparison of modeled and observed trends in indices of daily climate extremes, *J. Clim.*, *16*, 3560–3571.
- Meehl, G. A., and C. Tebaldi (2004), More intense, more frequent and longer lasting heat waves in the 21st century, *Science*, *305*, 994–997.

- Meehl, G. A., C. Tebaldi, and D. Nychka (2004), Changes in frost days in simulations of 21st century climate, *Clim. Dyn.*, *23*, 495–511.
- Meehl, G. A., W. M. Washington, W. D. Collins, J. M. Arblaster, A. Hu, L. E. Buja, W. G. Strand, and H. Teng (2005), How much more global warming and sea level rise?, *Science*, *307*, 1769–1772.
- Milly, P. C. D., R. T. Wetherald, K. A. Dunne, and T. L. Delworth (2002), Increasing risk of great floods in a changing climate, *Nature*, *415*, 514–517.
- Palmer, T. N., and J. Räisänen (2002), Quantifying the risk of extreme seasonal precipitation events in a changing climate, *Nature*, *415*, 512–514.
- Räisänen, J. (2005), Impact of increasing CO₂ on monthly to annual precipitation extremes: Analysis of the CMIP2 experiments, *Clim. Dyn.*, *24*, 309–323.
- Semenov, V. A., and L. Bengtsson (2002), Secular trends in daily precipitation characteristics: Greenhouse gas simulation with a coupled AOGCM, *Clim. Dyn.*, *19*, 123–140.
- Simmonds, I., D. Bi, and P. Hope (1999), Atmospheric water vapor flux and its association with rainfall over China in summer, *J. Clim.*, *12*, 1353–1367.
- Voss, R., W. May, and E. Roeckner (2002), Enhanced resolution modeling study on anthropogenic climate change: Changes in the extremes of the hydrological cycle, *Int. J. Climatol.*, *22*, 755–777.
- Watterson, I. G. (1998), An analysis of the global water cycle of present and doubled CO₂ climates simulated by the CSIRO general circulation model, *J. Geophys. Res.*, *103*, 23,113–23,129.
- Watterson, I. G., and M. R. Dix (2003), Simulated changes due to global warming in daily precipitation means and extremes and their interpretation using the gamma distribution, *J. Geophys. Res.*, *108*(D13), 4379, doi:10.1029/2002JD002928.
- Wehner, M. F. (2004), Predicted twenty-first-century changes in seasonal extreme precipitation events in the parallel climate model, *J. Clim.*, *17*, 4281–4290.
- Yin, J. H. (2005), A consistent poleward shift of the storm tracks in simulations of 21st century climate, *Geophys. Res. Lett.*, *32*, L18701, doi:10.1029/2005GL023684.
-
- J. M. Arblaster, G. A. Meehl, and C. Tebaldi, National Center for Atmospheric Research, P.O. Box 3000, Boulder, CO 80307, USA. (meehl@ncar.ucar.edu)